Journal of Power Sources 226 (2013) 54–60

Contents lists available at SciVerse ScienceDirect

Journal of Power Sources

journal homepage: www.elsevier.com/locate/jpowsour

High performance ceramic-coated separators prepared with lithium ion-containing SiO_2 particles for lithium-ion batteries

Won-Kyung Shin, Dong-Won Kim*

Department of Chemical Engineering, Hanyang University, Seungdong-Gu, Seoul 133-791, Republic of Korea

HIGHLIGHTS

- Core–shell SiO_2 particles are used as coating materials for ceramic-coated separators.
- The ceramic-coated separators exhibit good thermals stability and wettability.
- The cells assembled with ceramic-coated separators exhibit good cycling performance.

ARTICLE INFO

Article history:
Received 27 August 2012
Received in revised form
23 October 2012
Accepted 25 October 2012
Available online 6 November 2012

Keywords:
Ceramic-coated separators
Lithium-ion cells
Polyethylene separator
Sulfonated silica
Thermal stability

ABSTRACT

Sulfonated SiO_2 particles containing poly(lithium 4-styrenesulfonte) in their shell are synthesized and used as coating materials for the preparation of ceramic-coated separators for lithium-ion cells. The ceramic-coated separators exhibit good thermal stability and wettability for liquid electrolyte due to the presence of a heat-resistant silica with hydrophilic poly(lithium 4-styrenesulfonte). By using these ceramic-coated separators, lithium-ion cells composed of a carbon negative electrode and a $LiNi_{1/3}Co_{1/3}Mn_{1/3}O_2$ positive electrode are assembled and their cycling performances are evaluated. The cells assembled with the ceramic-coated separators demonstrate superior cycling performance compared to cell prepared with a polyethylene separator.

1. Introduction

The use of lithium-ion batteries has been rapidly expanding in portable electronic devices, plug-in hybrid electric vehicles (PHEVs), HEVs, EVs and energy storage systems due to their high energy density and long cycle life. In lithium-ion batteries, a separator is a critical component which prevents physical contact of the positive and negative electrodes while permitting free ionic transport within the cell. Most of the separators currently used in lithium-ion batteries are based on microporous polyolefin membranes such as polyethylene (PE) and polypropylene (PP) as well as various combinations of the two [1–3]. Although these separators offer excellent mechanical strength and chemical stability, they shrink, soften and even melt at high temperatures [4–6], which cause short circuiting between electrodes in the case of unusual heat generation. Furthermore, without surface treatment, the large difference in polarity between the non-polar polyolefin separator and the polar organic electrolyte leads to poor wettability [7,8]. As a result, there is a high resistance when the pores in the separator are not completely filled with liquid electrolyte. In order to solve these problems, ceramic-coated separators have been developed by combining the characteristics of a polymeric separator and ceramic materials [9–18]. In these separators, commercially available inorganic particles such as SiO_2 and Al_2O_3 have been coated with a polymer binder on a polyolefin separator. The coating of ceramic particles has been effective in improving the mechanical, thermal and electrical properties of separators only due to physical actions without directly contributing to the lithium ion transport process. In our previous studies, core–shell structured SiO_2 particles containing lithium ions in their shells were synthesized and used as functional fillers in Li^+-conducting composite polymer electrolytes [19,20]. These fillers are unique because the SiO_2 core is covalently bonded to poly(lithium 4-styrenesulfonte) (PLSS) in the shell layer. Thus, it is of great interest to introduce the SiO_2-based inorganic materials containing lithium ions to the ceramic-coated separator.

* Corresponding author. Tel.: +82 2 2220 2337; fax: +82 2 2298 4101.
E-mail address: dongwonkim@hanyang.ac.kr (D.-W. Kim).

0378-7753/$ – see front matter © 2012 Elsevier B.V. All rights reserved.
http://dx.doi.org/10.1016/j.jpowsour.2012.10.082

With the goal of developing high performance separators with high thermal stability, good transport properties and enhanced wettability for non-aqueous liquid electrolytes, we prepared ceramic-coated separators based on a PE separator and core–shell structured SiO_2 particles containing lithium ions. Due to the presence of a heat-resistant silica core with a hydrophilic shell component, the ceramic-coated separator exhibited good thermal stability and wettability for liquid electrolyte. Using these ceramic-coated separators, we assembled lithium-ion cells composed of a carbon negative electrode and a $LiNi_{1/3}Co_{1/3}Mn_{1/3}O_2$ positive electrode. The cycling performances of the cells assembled with the ceramic-coated separator were evaluated as a function of the core–shell SiO_2 content and the results were compared to those obtained with a pristine PE separator.

2. Experimental

2.1. Synthesis of core–shell structured SiO_2 particles

The core–shell structured $SiO_2(Li^+)$ particles were synthesized through three steps, as reported earlier [19]. Vinyltrimethoxysilane (VTMS) was added to double distilled water under stirring for 30 min until the VTMS droplets completely disappeared. A catalytic amount of NH_4OH was then added to the solution and the reaction was continued for 12 h at room temperature. After completion of the reaction, the resulting precipitate was centrifuged and washed several times with ethanol. Core–shell $SiO_2(Na^+)$ particles were synthesized by radical copolymerization of silica core particles with 4-styrenesulfonic acid sodium salt. The silica core particles were dispersed in *n*-methyl pyrrolidone (NMP) via ultrasonication for 30 min and a solution consisting of 4-styrenesulfonic acid sodium salt and azobisisobutyronitrile (AIBN) dissolved in NMP was added. To induce polymerization, the mixture was heated to 60 °C under stirring for 72 h. After polymerization, the solution was precipitated in excess diethyl ether under vigorous stirring. The precipitate was filtered and washed several times with methanol/ethanol. The Na^+ ions in the core–shell structured $SiO_2(Na^+)$ particles were replaced by Li^+ ions by ionic exchange with $LiOH \cdot H_2O$ [21]. The resulting core–shell $SiO_2(Li^+)$ powders were washed with ethanol to remove any impurities and dried under vacuum at 110 °C for 12 h.

2.2. Preparation of the ceramic-coated separator

Ceramic-coated separators were prepared from the core–shell $SiO_2(Li^+)$ particles and poly(vinylidene fluoride-co-hexafluoropropylene) (P(VdF-co-HFP), Kynar 2801) as a polymer binder. P(VdF-co-HFP) was dissolved in an acetone/butanol solvent mixture (90/10 by volume), and the core–shell $SiO_2(Li^+)$ particles were directly added to the polymer solution at concentrations of 0, 10, 20, and 30 wt.%. The slurry was uniformly mixed by ball milling for 24 h. Using a dip coating method, the resulting slurry was then coated onto both sides of a microporous PE separator (Asahi-Kasei Co.) with a thickness of 20 μm and a porosity of 40%. Next, the separator was dried at room temperature for 10 min to allow the solvent to evaporate, followed by additional drying in a vacuum oven at 60 °C for 24 h. The coating thickness was adjusted by changing the content of the $SiO_2(Li^+)$ particles and P(VdF-co-HFP) in the slurry so that the total thickness of the ceramic-coated separator was kept to be about 29 μm.

2.3. Electrode preparation and cell assembly

The positive electrode was prepared by coating the N-methyl pyrrolidine (NMP)-based slurry containing 85 wt.% $LiNi_{1/3}Co_{1/3}Mn_{1/3}O_2$ (3 M), 7.5 wt.% poly(vinylidene fluoride)(PVdF), and 7.5 wt.% super-P carbon (MMM Co.) on an aluminum foil. After vacuum drying, the electrode was punched into a disk. A geometrical area of the positive electrode was 1.54 cm^2, and its active mass loading corresponded to a capacity of about 2.0 mAh cm^{-2}. The negative electrode was prepared similarly by coating the NMP-based slurry of mesocarbon microbeads (MCMB, Osaka gas), PVdF and super-P carbon at a weight ratio of 85/7.5/7.5 on a copper foil. The negative electrode was also cut into a disk with a geometric area of 2.01 cm^2. Lithium-ion cells were assembled by sandwiching the ceramic-coated separator between the carbon electrode and the $LiNi_{1/3}Co_{1/3}Mn_{1/3}O_2$ electrode. The cell was then enclosed in a 2032 coin cell and injected with the same amount of electrolyte solution, which consisted of 1.15 M $LiPF_6$ in ethylene carbonate (EC)/diethyl carbonate (DEC) (3:7 by volume, Soulbrain Co. Ltd.). The nominal capacity of coin cell was about 3.1 mAh, and thus 1C rate corresponded to 3.1 mA. All cells were assembled in a dry box filled with argon gas.

2.4. Measurements

The morphologies of the materials were examined using a field emission scanning electron microscope (FE-SEM, JEOL JSM-6330F) and a field emission transmission electron microscope (FE-TEM, FEI, Tecnai G2 F30). Fourier transform infrared (FT-IR) spectra were recorded on a Magna IR 760 spectrometer in the range of 400-4000 cm^{-1} with KBr powder-pressed pellets. The presence of lithium ions in the core–shell structured SiO_2 particles was confirmed by Auger Electron Spectroscopy (AES, ULVAC-PHI, PHI 700). The thermal shrinkage of the ceramic-coated separators in the form of their dimensional change was measured before and after being held at 130 °C for 30 min. The internal short circuit temperature of the cell was determined as the temperature which showed a sudden voltage drop, as the temperature of the cell was increased. In order to measure the electrolyte uptake and ionic conductivity, the ceramic-coated separator was immersed in the 1.15 M $LiPF_6$ in EC/DEC solution for 1 h. Afterward, the separator was taken out from the electrolyte solution and the excess electrolyte solution on the surface of separator was removed by wiping with filter paper. The uptake of the electrolyte solution was then determined by using equation (1),

$$\text{uptake}\ (\%) = (W - W_o)/W_o \times 100 \quad (1)$$

where W_o and W are the weights of the separator before and after soaking in the liquid electrolyte, respectively [22–24]. The wetted separator was sandwiched between two stainless steel electrodes for conductivity measurements. AC impedance measurements were performed to measure the ionic conductivity using an impedance analyzer over the frequency range of 10 Hz–100 kHz with amplitude of 10 mV. Charge and discharge cycling tests of the lithium-ion cells were conducted at a current of 1.55 mA (0.5 C rate) over a voltage range of 3.0–4.5 V using battery test equipment.

3. Results and discussion

Fig. 1(a) shows an FE-SEM image of the silica core particles. The particles have a uniform spherical shape with particle size ranging from 790 to 830 nm. From the FT-IR spectra of the silica core particles, peaks corresponding to the siloxane (Si–O–Si) group (766, 1000–1200 cm^{-1}) and C=C double bonds (1410, 1603 cm^{-1}) were observed [19]. These results imply that the silica core particles contain reactive vinyl groups which permit the growth of silica particles by radical polymerization with 4-styrenesulfonic acid sodium salt. Core-shell structured SiO_2 particles were obtained by

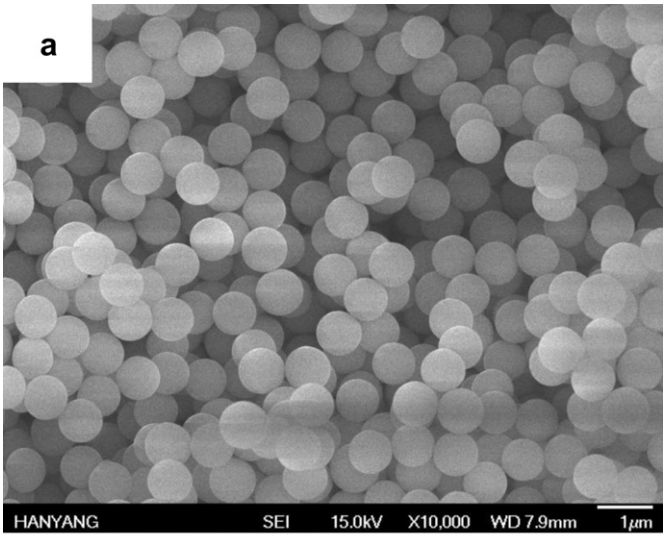

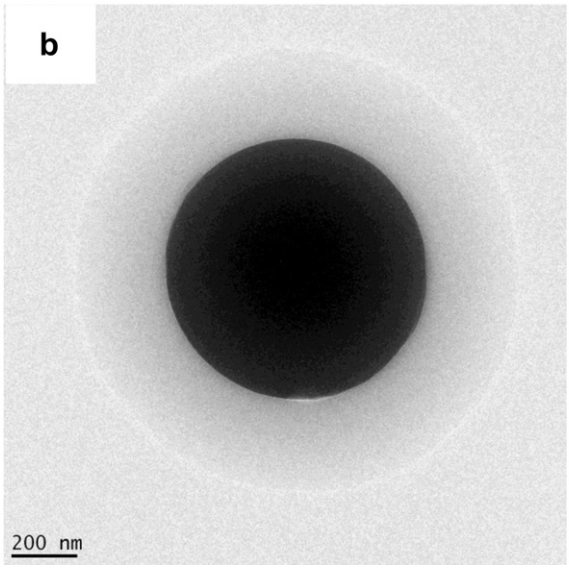

Fig. 1. (a) FE-SEM images of silica particles and (b) a core–shell SiO_2 particle containing PSSS in the shell.

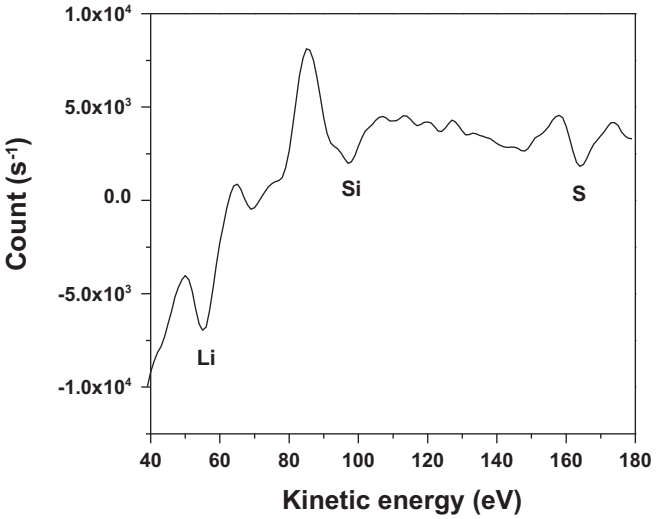

Fig. 2. AES profile of core–shell $SiO_2(Li^+)$ particles. The peaks corresponding to lithium, silicon, and sulfur are shown in the figure.

radical copolymerization of silica core particles and 4-styrenesulfonic acid sodium salt. Fig. 1(b) shows a TEM image of a core–shell silica particle containing poly(sodium 4-styrenesulfonte) (PSSS) in the shell. The particle has very uniform core–shell morphology with a 290 nm thick shell layer of PSSS (gray) surrounding a SiO_2 core particle (black). The core diameter is estimated to be about 810 nm, which is consistent with the image in Fig. 1(a). This result indicates that the spherical SiO_2 particles are well encapsulated by PSSS with a uniform thickness. Using these core–shell structured $SiO_2(Na^+)$ particles, we replaced the sodium ions in the shells of the core–shell structured SiO_2 particles with lithium ions. The AES profile of the core–shell structured $SiO_2(Li^+)$ particles shown in Fig. 2 reveals a 54.8 eV characteristic peak corresponding to lithium [25], confirming that the $SiO_2(Na^+)$ particles are converted to $SiO_2(Li^+)$ particles.

FE-SEM images of the surface of the porous PE separator and ceramic-coated separator are presented in Fig. 3. The PE separator exhibits a uniformly interconnected submicron pore structure. As the core–shell $SiO_2(Li^+)$ particles with polymer binder are coated onto the PE substrate, the particles are homogeneously distributed in the surface layer without agglomeration. The presence of the coating layer consisting of core–shell $SiO_2(Li^+)$ particles and P(VdF-co-HFP) is expected to improve the thermal stability of the PE separator and also enhance the wettability for liquid electrolyte upon immersion in an electrolyte solution.

In order to evaluate the heat-resistant properties of the ceramic-coated separators, we measured the thermal shrinkage after storing the separators at 130 °C for 30 min, and the results are given in Table 1 and Fig. 4. As shown in Fig. 4, the PE separator exhibits a high degree of shrinkage (16.3%) during exposure to the high temperature conditions. Since the manufacturing process of microporous PE separators includes a drawing step, the PE separator easily shrinks when exposed to high temperature [2], which may result in physical contact between negative electrode and positive electrode. On the other hand, the thermal shrinkage was remarkably reduced by coating both sides of the PE separator with core–shell $SiO_2(Li^+)$ particles and polymer binder. It is considered that the coating of ceramic-based particles onto both sides of the PE separator can prevent dimensional changes by thermal deformation because of the frame structure of the heat-resistant ceramic powder with polymer binder. The separators used in lithium-ion batteries should have also high temperature melt integrity, which helps to avoid thermal runaway when the cell is exposed to high temperatures. This is especially important for large scale lithium-ion cells being developed for electric vehicles and energy storage systems. Internal short circuits are evidenced by precipitous drops in the cell voltage, and the internal short circuit temperatures which corresponded to sudden voltage drops are given in Table 1. The cell with a conventional PE separator shows an internal short circuit at 130 °C. On the contrary, the cells assembled with the ceramic-coated separator exhibit a sudden voltage drop at around 160 °C, suggesting the coating layer containing core–shell $SiO_2(Li^+)$ particles on the outside of the PE separator helps in maintaining the melt integrity of the separator at higher temperatures.

The wettability of the separator plays an important role in battery performance because the separator with good wettability can effectively retain the electrolyte solution and facilitate ion transport between electrodes [1,2]. The electrolyte uptake is one of the indicators for the wettability of the separator. The uptake of organic electrolyte in the ceramic-coated separator and the ionic conductivity after soaking in the liquid electrolyte were measured and are summarized in Table 1. For comparison purposes, a pristine

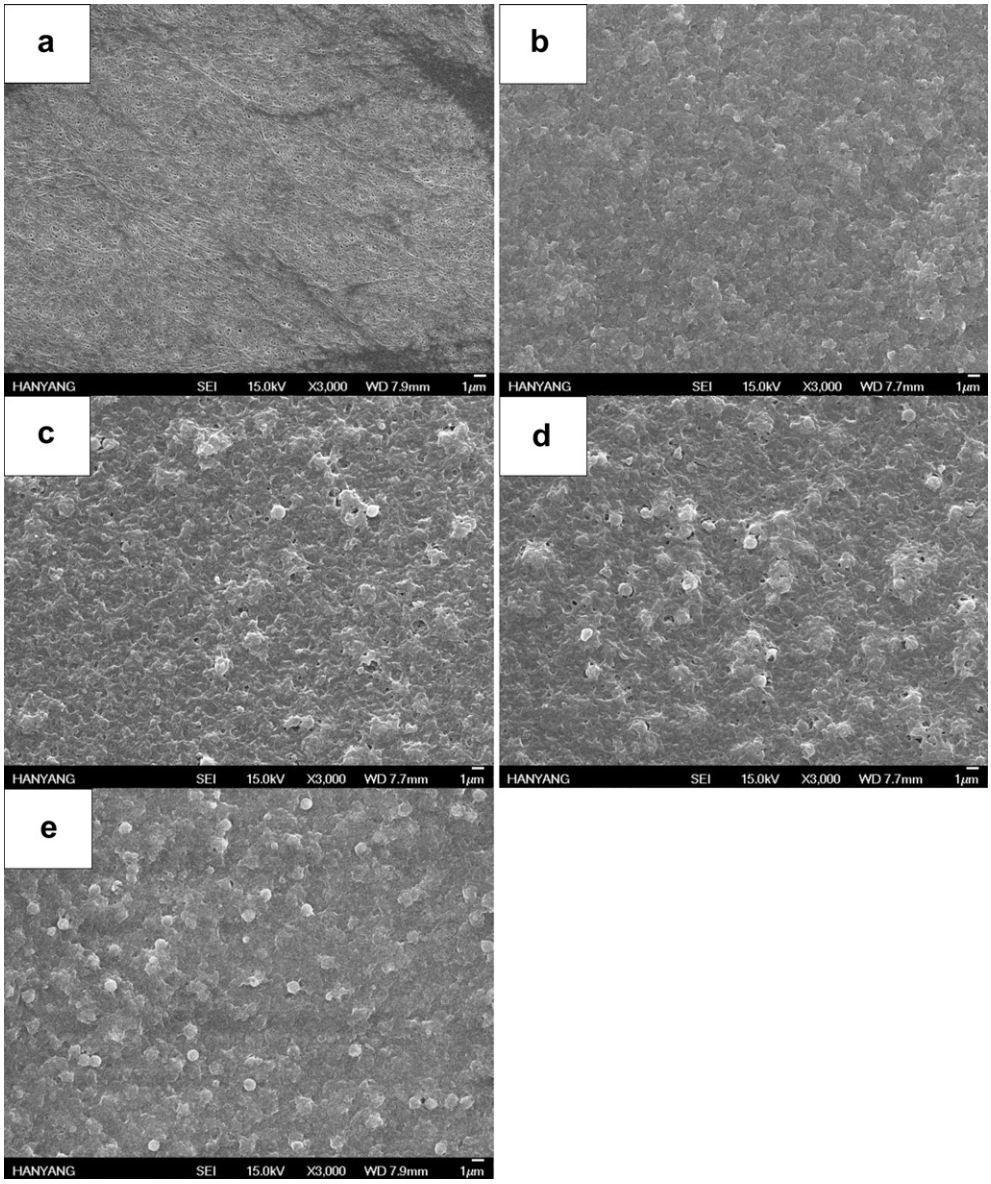

Fig. 3. FE-SEM images of the surface of a pristine PE separator and ceramic-coated separators containing different amounts of $SiO_2(Li^+)$ particles: (a) PE separator, and ceramic-coated separators containing (b) 0 wt.%, (c) 10 wt.%, (d) 20 wt.%, and (e) 30 wt.% $SiO_2(Li^+)$ particles.

PE separator was soaked in the same electrolyte solution and the corresponding results are included in Table 1. The ionic conductivity of the liquid electrolyte used in soaking the separators is 6.0×10^{-3} S cm^{-1} at room temperature. It can be seen that the ionic conductivity of the PE separator filled with the electrolyte solution is lower than that of the electrolyte solution, which is due to the fact that the specific resistivity of the separator saturated with liquid electrolyte is increased due to the combination of the tortuosity and porosity of the separator [1]. The PE separator exhibits poor wettability due to its inherent hydrophobic properties. For the ceramic-coated separators, the amount of electrolyte absorbed is greater than the amount absorbed by the PE separator, which results in a higher ionic conductivity. This is due to the fact that the hydrophilic PLSS in the shell of the core–shell structured

Table 1
Physical properties of the PE separator and ceramic-coated separators containing different amounts of $SiO_2(Li^+)$ particles.

Separator	Thickness (μm)	Thermal shrinkage (%)	Internal short temperature (°C)	Electrolyte uptake (%)	Ionic conductivity (S cm^{-1})
PE	20	16.3	130	97.6	3.9×10^{-4}
$SiO_2(Li^+)$ 0 wt.%	29	9.8	150	157.6	5.4×10^{-4}
$SiO_2(Li^+)$ 10 wt.%	29	7.9	160	212.2	7.2×10^{-4}
$SiO_2(Li^+)$ 20 wt.%	29	5.9	160	231.7	7.9×10^{-4}
$SiO_2(Li^+)$ 30 wt.%	29	4.0	160	242.8	7.5×10^{-4}

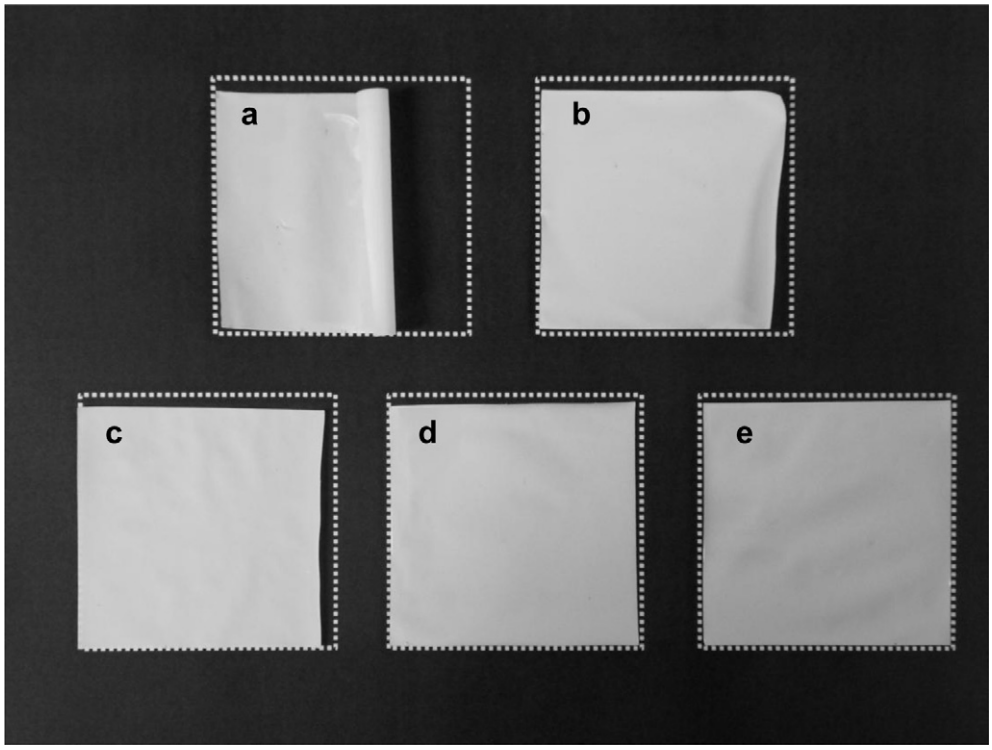

Fig. 4. Photographs of (a) a PE separator and ceramic-coated separators containing (b) 0 wt.%, (c) 10 wt.%, (d) 20 wt.%, and (e) 30 wt.% $SiO_2(Li^+)$ particles after being held at 130 °C for 30 min.

$SiO_2(Li^+)$ particles has a high affinity for the electrolyte solution. As a result, the liquid electrolyte is not only encapsulated in the pores but also retained in the coating layer composed of the $SiO_2(Li^+)$ particles and P(VdF-co-HFP). The lithium ions dissociated from the $SiO_2(Li^+)$ particles can also contribute to the ionic conductivity, resulting in the increasing ionic conductivity with increasing $SiO_2(Li^+)$ content [19,20]. The decrease of the ionic conductivity beyond 20 wt.% $SiO_2(Li^+)$ may be attributed to the blocking effect of the charge carrier transport since the core of the $SiO_2(Li^+)$ powder is an insulator by nature.

We evaluated the cycling performance of lithium-ion cells prepared with the ceramic-coated separator. The cells were initially subjected to a preconditioning cycle in the voltage range of 3.0–4.5 V at constant current rates of 0.05 C, 0.1 C, and 0.2 C, consecutively. After three cycles, the cells were charged at a current density of 0.5 C rate up to a target voltage of 4.5 V. This was followed by a constant voltage charge with declining current until a final current equal to 20% of the charging current was obtained. The cells were then discharged to a cut-off voltage of 3.0 V at the same current density. Fig. 5 shows the charge–discharge curves of the 1st, 10th, 20th, 50th, and 100th cycle of the lithium-ion cell assembled with the ceramic-coated separator containing 20 wt.% $SiO_2(Li^+)$. The cell delivers an initial discharge capacity of 173.5 mAh g^{-1} based on the active $LiNi_{1/3}Co_{1/3}Mn_{1/3}O_2$ material in the positive electrode. The discharge capacity of the cell declines to 155.4 mAh g^{-1} after 100 charge/discharge cycles. Fig. 6 shows the discharge capacities of lithium-ion cells assembled with different separators as a function of the cycle number. It has been reported that the presence of an additional coating layer on the porous PE separator increased the resistance of ion migration in the separator, giving rise to a reduced discharge capacity [10,16]. However, in the present study, the initial discharge capacity of the cell is slightly increased by coating the PE separator with $SiO_2(Li^+)$ powder and polymer binder, resulting from the improved ionic conductivity after coating $SiO_2(Li^+)$ powder and polymer binder onto both sides of the PE separator, as shown in Table 1. The capacity retention is also improved by using the ceramic-coated separator. The ability to retain electrolyte solution in the ceramic-coated separator is higher than in the hydrophobic PE separator and thus helps to prevent a leak of electrolyte during repeated cycling. When examining the effect of the content of the $SiO_2(Li^+)$ powder on the cell performance, the cell assembled with the ceramic-coated separator containing a higher content of $SiO_2(Li^+)$ exhibits a better capacity retention. Capacity fading in Fig. 6 seems to be fast as compared to those of previous works by Yabuuchi et al. [26,27], although the

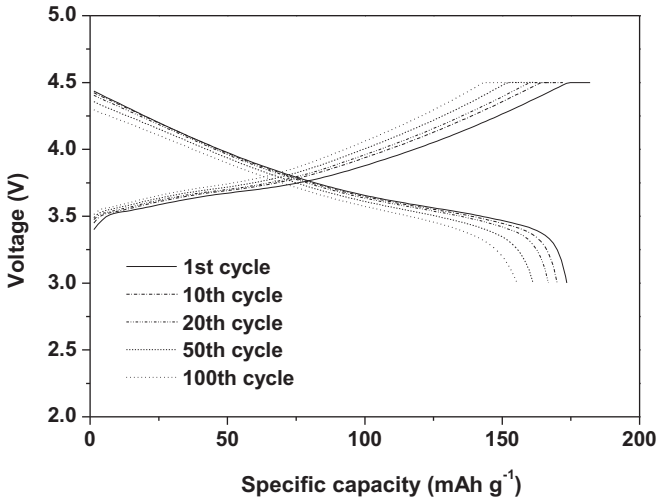

Fig. 5. Charge and discharge curves of lithium-ion cell assembled with the ceramic-coated separator containing 20 wt.% $SiO_2(Li^+)$ particles (0.5 C CC & CV charge, 0.5 C CC discharge, cut-off of 3.0–4.5 V).

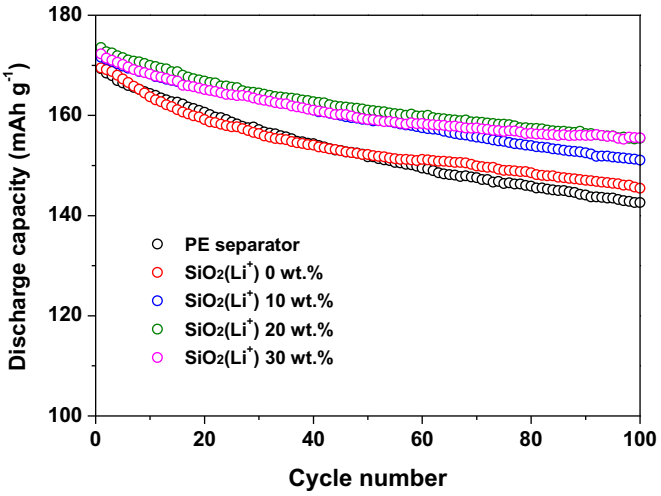

Fig. 6. Discharge capacities of the lithium-ion cells prepared with a PE separator and ceramic-coated separators (0.5 C CC & CV charge, 0.5 V CC discharge, cut-off of 3.0–4.5 V).

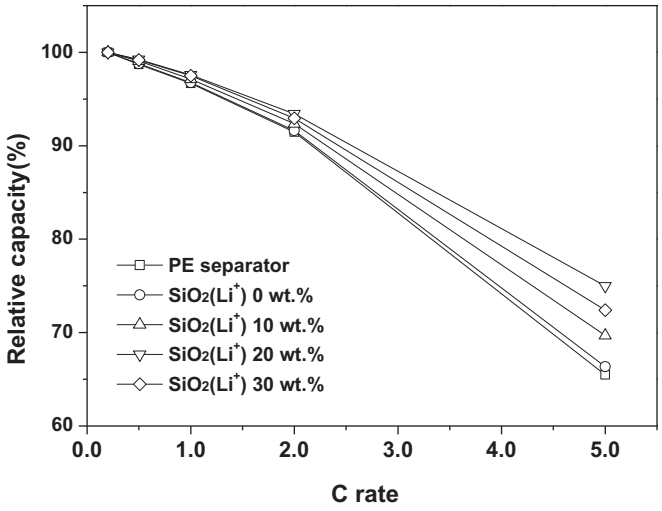

Fig. 8. Relative capacities of lithium-ion cells prepared with a PE separator and ceramic-coated separators as a function of the C rate.

capacity retention is improved by using the ceramic-coated separator. The capacity fading may be due to the imbalance of coulombic efficiencies between the negative and positive electrodes [28]. High cut-off voltage (4.5 V) for charging can also cause a gradual degradation of capacity, based on earlier report that charge-end voltage should be set below 4.4 V to avoid a capacity fading due to the change in lattice volume [27].

The rate capability of the lithium-ion cell prepared with the ceramic-coated separator was also evaluated. Cells were charged to 4.5 V at a constant current of 0.2 C and discharged at different current rates ranging from 0.2 to 5.0 C. The discharge curves of the lithium-ion cell assembled with the ceramic-coated separator containing 20 wt.% $SiO_2(Li^+)$ are given in Fig. 7. Fig. 8 compares the relative discharge capacities of lithium-ion cells prepared with different separators as a function of the current density, where the relative capacity is defined as the ratio of the discharge capacity at a specific C rate to the discharge delivered at a rate of 0.2 C. The results demonstrate that the rate capability of the cell is improved by coating the PE separator with $SiO_2(Li^+)$ powder and polymer binder. The coating layer on both sides of the PE separator assists the adhesion of the separator to the electrodes after soaking in the electrolyte solution, which results in favorable interfacial charge transport between the electrodes and electrolytes in the cell. In the case of the ceramic-coated separator containing 30 wt.% $SiO_2(Li^+)$, the excessive $SiO_2(Li^+)$ particles in the separator decrease the ionic conductivity, as given in Table 1, the result of which is a decreased discharge capacity at high current rates.

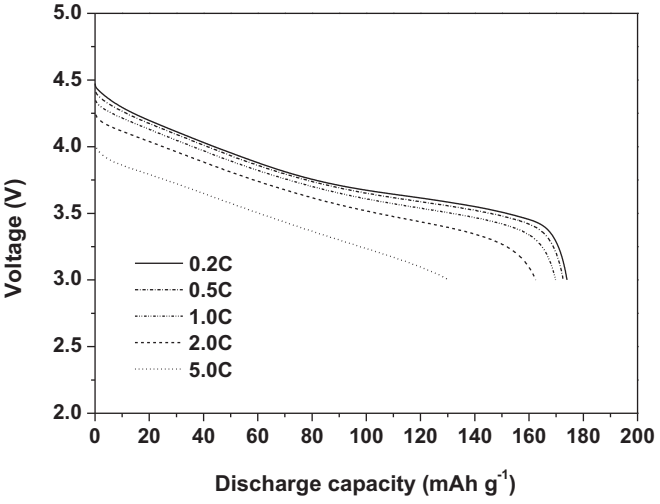

Fig. 7. Discharge profiles of the lithium-ion cell prepared with a ceramic-coated separator containing 20 wt.% $SiO_2(Li^+)$ particles as function of the C rate. The charge rate was 0.2 C with a 4.5 V cut-off.

4. Conclusions

Core–shell structured SiO_2 particles containing Li^+ ions in their shell are synthesized. The ceramic-coated separators are prepared by coating the core–shell $SiO_2(Li^+)$ particles and P(VdF-co-HFP) onto both sides of a porous PE separator. These separators have enhanced thermal stability and melt integrity. Due to the hydrophilic PLSS in the shell of the $SiO_2(Li^+)$ particles, the ceramic-coated separators exhibit good wettability for liquid electrolytes and high ionic conductivity. As a result, the lithium-ion cells assembled with the ceramic-coated separators exhibit better cycling performance than the cells prepared with a pristine PE separator. The results reported in this work encourage us to continue the study of lithium-ion polymer batteries with the aim of further improving cycling performance by optimizing the ceramic-coated separator with respect to thickness and porosity of coating layer, core size and shell thickness of core–shell SiO_2 particle.

Acknowledgment

This research was supported by a grant from the Fundamental R&D Program for Core Technology of Materials and the Human Resources Development of KETEP Grant funded by the Korea government Ministry of Knowledge Economy (No. 20104010100560).

References

[1] P. Arora, Z. Zhang, Chem. Rev. 104 (2004) 4419–4462.
[2] S.S. Zhang, J. Power Sources 164 (2007) 351–364.
[3] D. Linden, T.B. Reddy, Handbook of Batteries, third ed., McGraw-Hill, New York, 2002.
[4] I. Uchida, H. Ishikawa, M. Mohamedi, M. Umeda, J. Power Sources 119–121 (2003) 821–825.
[5] G. Venugopal, J. Moore, J. Howard, S. Pendalwar, J. Power Sources 77 (1999) 34–41.
[6] M.S. Wu, P.C.J. Chiang, J.C. Lin, Y.S. Jan, Electrochim. Acta 49 (2004) 1803–1812.

[7] J. Saunier, F. Alloin, J.Y. Sanchez, G. Caillon, J. Power Sources 119–121 (2003) 454–459.
[8] Y.M. Lee, J.W. Kim, N.S. Choi, J.A. Lee, W.H. Seol, J.K. Park, J. Power Sources 139 (2005) 235–241.
[9] H.S. Jeong, D.W. Kim, Y.U. Jeong, S.Y. Lee, J. Power Sources 195 (2010) 6116–6121.
[10] J.A. Choi, S.H. Kim, D.W. Kim, J. Power Sources 195 (2010) 6192–6196.
[11] Y.S. Lee, Y.B. Jeong, D.W. Kim, J. Power Sources 195 (2010) 6197–6201.
[12] M. Kim, G.Y. Han, K.J. Yoon, J.H. Park, J. Power Sources 195 (2010) 8302–8305.
[13] J.H. Park, J.H. Cho, W. Park, D. Ryoo, S.J. Yoon, J.H. Kim, Y.U. Jeong, S.Y. Lee, J. Power Sources 195 (2010) 8306–8310.
[14] H.S. Jeong, S.C. Hong, S.Y. Lee, J. Membr. Sci. 364 (2010) 177–182.
[15] H.S. Jeong, J.H. Noh, C.G. Hwang, S.H. Kim, S.Y. Lee, Macromol. Chem. Phys. 211 (2010) 420–425.
[16] H.S. Jeong, S.Y. Lee, J. Power Sources 196 (2011) 6716–6722.
[17] X. Huang, J. Power Sources 196 (2011) 8125–8128.
[18] D. Fu, B. Luan, S. Argue, M.N. Bureau, I.J. Davidson, J. Power Sources 206 (2012) 325–333.
[19] Y.S. Lee, S.H. Ju, J.H. Kim, S.S. Hwang, J.M. Choi, Y.K. Sun, H. Kim, B. Scrosati, D.W. Kim, Electrochem. Commun. 17 (2012) 18–21.
[20] Y.S. Lee, J.H. Lee, J.A. Choi, W.Y. Yoon, D.W. Kim, Adv. Funct. Mater. (2012). http://dx.doi.org/10.1002/adfm.201200692.
[21] C.H. Park, Y.K. Sun, D.W. Kim, Electrochim. Acta 50 (2004) 375–378.
[22] J.R. Kim, S.W. Choi, S.M. Jo, W.S. Lee, B.C. Kim, J. Electrochem. Soc. 152 (2005) A295–A300.
[23] X. Li, G. Cheruvally, J.K. Kim, J.W. Choi, J.H. Ahn, K.W. Kim, H.J. Ahn, J. Power Sources 167 (2007) 491–498.
[24] Y. Ding, P. Zhang, Z. Long, Y. Jiang, F. Xu, W. Di, J. Membr. Sci. 329 (2009) 56–59.
[25] M.P. Seah, D. Briggs, Practical Surface Analysis by Auger and X-ray Photoelectron Spectroscopy, second ed., Wiley & Sons, 1992.
[26] N. Yabuuchi, T. Ohzuku, J. Power Sources 119–121 (2003) 171–174.
[27] N. Yabuuchi, Y. Makimura, T. Ohzuku, J. Electrochem. Soc. 154 (2007) A314–A321.
[28] T. Ohzuku, A. Ueda, N. Yamamoto, Y. Iwakoshi, J. Power Sources 54 (1995) 99–102.